

See discussions, stats, and author profiles for this publication at: <https://www.researchgate.net/publication/316934530>

# Lightning as a Source of Electricity: Atmospheric Modeling of Electromagnetic Fields

Article in *International Journal of Technology* · April 2017

DOI: 10.14716/ijtech.v8i3.5783

---

CITATIONS

0

---

READS

62

Some of the authors of this publication are also working on these related projects:



Environmental Engineering- Solution for air pollution [View project](#)



RENEWABLE ENERGY PROSPECTS IN DEVELOPING COUNTRIES [View project](#)

## LIGHTNING AS A SOURCE OF ELECTRICITY: ATMOSPHERIC MODELING OF ELECTROMAGNETIC FIELDS

Moses Eterigho Emetere<sup>1\*</sup>

<sup>1</sup>*Department of Physics, Covenant University Canaan Land, P.M.B 1023, Ota, 122333, Nigeria*

(Received: September 2016 / Revised: February 2017 / Accepted: April 2017)

### ABSTRACT

A weather- influenced Maxwell's electromagnetic model for lightning activities has been considered. Three governing equations were stated for further analysis. The charge dynamics, lightning branches and atmospheric factors were analyzed. The model was validated by analyzing ground data from the Davis-Pro weather station. The data collected was targeted for the month with the highest lightning activity. It was discovered that lightning occurs at the upper pressure level (under certain conditions that are stated in the thesis) while the low pressure level initiates an updraft, i.e. air rises and condenses into a cumulonimbus cloud. These findings present the keys to considering a lightning system as a source of alternative energy.

*Keywords:* Davis weather station; Electricity; Electromagnetic model; Lightning

### 1. INTRODUCTION

An in-depth analysis of lightning electric and magnetic fields have been explained by a few models like gas-dynamic models, electromagnetic models, distributed-circuit models, engineering models, etc. However, the errors noticed in the various models have informed a proactive effort to address the shortcomings of these models in practical applications. Many of the anomalies in lightning models have been due to aerosol loadings (Emetere et al., 2015a). Primarily, most lightning electromagnetic models involve a numerical solution of Maxwell's equations to investigate its magnetic effects and the corresponding change in the current distribution along the lightning channel. The validity of the current distribution has attracted further arguments (Baba et al., 2005) especially as regards to the transverse electromagnetic (TEM) and the non-transverse electromagnetic (NTEM) data. One of the vital advantages of the current distribution along the lightning channel is the investigation and prediction of deleterious coupling of lightning fields, as it has-over the years affected various electric systems. Understanding the deleterious coupling of lightning fields is practically synonymous to the return stroke concept.

From basic knowledge of lightning, the return stroke travels via a path known as channel. The return stroke channel acts as a conducting pathway for the current wave propagation, with the source being located at the ground. The theory of the return stroke concept has deluded most experimentalists as different measuring devices (Hussein et al., 2007; Rachidi et al., 2004; Tatematsu et al., 2004; Emetere et al., 2015a) had shown varying results. The sensitivity of the measuring devices are in no way relevant anymore as the prevailing global weather change alters charged particulate mobility both in the atmosphere and near earth surface (Emetere et al., 2015a; Emetere et al., 2015b).

---

\*Corresponding author's email: emetere@yahoo.com, Tel. +234-8035267598, Fax. +234-8035267598  
Permalink/DOI: <https://doi.org/10.14716/ijtech.v8i3.5783>

Therefore, the ab-initio concept of electromagnetism i.e. the Maxwell's equations needs to be revised to incorporate some salient global weather terms to capture-adequately the concept of return stroke (Emetere et al., 2015a). The objective of this paper is to show both mathematically and experimentally the abnormalities in the return stroke concept. The advantage of the paper is to initiate the mathematical framework of a lightning tracker panel.

In the past, cogent work has been done by solving Maxwell's based model (Miller et al., 1973; Rakov & Uman, 1998) to dissolve a few of the mysteries of the return stroke concept. For example, the transmission line (TL) model was used to demonstrate the reproducibility of return strokes within microseconds (Schoene et al., 2003). The transmission model, as explained by Uman and McLain (1969) entails monitoring current wave injected at the bottom of the lightning channel that is traveling upward (return stroke) at constant velocity without signal scattering, attenuation or distortion, though in fact many authors have worked on the assumption-that the current wave signals do not attenuate (Lupo et al., 2000; Schoene et al., 2003). In this paper, the theories of cloud-to-ground lightning were discussed so as to provide a mathematical framework of harnessing the potential of lightning as an alternative energy source.

## 2. THEORIES OF CLOUD-TO-GROUND LIGHTNING

The ab-initio calculations of Uman and McLain (1969), the horizontal, vertical and azimuth magnetic fields of the electromagnetic model are given in integral form in Equations 1–3, respectively below.

$$E_r(r, z, t) = \frac{1}{4\pi\epsilon_0} \left[ \int_{-H}^H \frac{3r(z-z^\top)}{R^5} \int_0^t i(z^\top, \tau - R/c) d\tau dz^\top + \int_{-H}^H \frac{3r(z-z^\top)}{cR^4} i(z^\top, \tau - R/c) dz + \int_{-H}^H \frac{r^2}{c^2 R^3} \frac{\partial i(z^\top, \tau - R/c)}{\partial t} dz^\top \right] \quad (1)$$

$$E_z(r, z, t) = \frac{1}{4\pi\epsilon_0} \left[ \int_{-H}^H \frac{2(z-z^\top)^2 - r^2}{R^5} \int_0^t i(z^\top, \tau - R/c) d\tau dz^\top + \int_{-H}^H \frac{2(z-z^\top)^2 - r^2}{cR^4} i\left(z^\top, \tau - \frac{R}{c}\right) dz^\top - \int_{-H}^H \frac{r(z-z^\top)}{c^2 R^3} \frac{\partial i(z^\top, \tau - R/c)}{\partial t} dz^\top \right] \quad (2)$$

$$B_\phi(r, z, t) = \frac{\mu_0}{4\pi} \left[ \int_{-H}^H \frac{r}{R^3} i\left(z^\top, \tau - \frac{R}{c}\right) dz^\top + \int_{-H}^H \frac{r}{cR^2} \frac{\partial i(z^\top, \tau - R/c)}{\partial t} dz^\top \right] \quad (3)$$

$r$ , is the horizontal distance between the channel and the observation point ;  $\epsilon_0$  is the permittivity of the vacuum;  $c$ , is the speed of light;  $\mu_0$  is the permeability of the vacuum;  $R$ , is the distance from the dipole to the observation point,  $\tau$  is the front time constant and  $i(z^\top, t)$  is the current carried by the  $dz'$  dipole at time  $t$ .

The mixing ratio ( $q_x$ ) of the cloud microphysics particles ( $x$ ) are governed by the continuity equation of mass, which can be expressed as a balance of the advection ( $q_{xa}$ ), turbulence ( $q_{xt}$ ), sources ( $q_{xs}$ ) and sinks ( $q_{xd}$ ) of the hydrometeors. We shall be considering the one-dimensional cloud microphysics model, as shown in Equation 4, where:

$$\frac{\partial q_x}{\partial t} = \frac{\partial q_{xa}}{\partial t} + \frac{\partial q_{xt}}{\partial t} + \frac{\partial q_{xs}}{\partial t} + \frac{\partial q_{xd}}{\partial t} \quad (4)$$

Also, the electric charge density mixing ( $Q_x$ ) for the different parameters listed above is given as shown in Equation 5:

$$\frac{\partial Q_x}{\partial t} = \frac{\partial Q_{xa}}{\partial t} + \frac{\partial Q_{xt}}{\partial t} + \frac{\partial Q_{xs}}{\partial t} + \frac{\partial Q_{xd}}{\partial t} \quad (5)$$

The neutralization of the charges from these sources had already been reported by Ziegler and MacGorman (1994) as shown in Equation 6:

$$\frac{\partial Q_{net}}{\partial t} = \begin{cases} 0 & \text{if } \frac{\partial Q_{net}}{\partial t} \leq \frac{\partial Q_{th}}{\partial t} \\ \left( \left| \frac{\partial Q_{net}}{\partial t} \right| - \frac{\partial Q_{th}}{\partial t} \right) f_p - \frac{\partial Q_{cor}}{\partial t} & \text{if } \frac{\partial Q_{net}}{\partial t} < -\frac{\partial Q_{th}}{\partial t} \\ -\left( \frac{\partial Q_{net}}{\partial t} - \frac{\partial Q_{th}}{\partial t} \right) f_p - \frac{\partial Q_{cor}}{\partial t} & \text{if } \frac{\partial Q_{net}}{\partial t} > -\frac{\partial Q_{th}}{\partial t} \end{cases} \quad (6)$$

where  $\frac{\partial Q_{net}}{\partial t}$  is the net rate of charge density before the lightning,  $\frac{\partial Q_{th}}{\partial t} \approx Q_{th}$  is a threshold,  $f_p$  is the fraction to be neutralized and  $\frac{\partial Q_{cor}}{\partial t}$  is a correction to guarantee that same amount of negative and positive charges are neutralized as shown in Equation 7:

$$\frac{\partial Q_x}{\partial t} = \frac{\sigma_x}{\sum \sigma_x} \frac{\partial Q_{net}}{\partial t} \quad (7)$$

where  $\sigma_x$  represents the spheres of the charged particulate and given as  $\sigma_x = 2\pi r_x^2$ .  $r_x$  is the radius of the sphere. The production of positive and negative charged particulates in the atmosphere is mathematically represented by Srivastava and Tripathi (2010). The time dependent conservation equation for positive ions and negative ions are represented, respectively in Equations 8a & 8b as shown below:

$$\frac{dn_1}{dt} = q - \alpha n_1 n_2 - \beta_1 (S n_1 + S_2 n_1) - \frac{1}{e} \nabla J_{z1} \quad (8a)$$

$$\frac{dn_2}{dt} = q - \alpha n_1 n_2 - \beta_2 (S n_2 + S_1 n_2) - \frac{1}{e} \nabla J_{z2} \quad (8b)$$

where  $n_{1,2}$  are positive (negative) ion concentrations,  $\beta_{1,2}$  are positive (negative) ion attachment coefficients with droplets,  $S_{1,2}$  that are charged droplet concentrations having unit positive (negative) charge,  $S$  is the neutral droplet concentrations,  $e$  is the electronic charge,  $q$  is the ion production rate,  $\alpha$  is the ion-ion recombination coefficient and  $\nabla J_{z1,2}$  is vertical current density. The charge dynamics between the cloud and ground is adopted from the Navier-Stokes equation, i.e. as shown in Equation 9:

$$\frac{\partial u}{\partial t} + (u \cdot \nabla) u + \nabla p = \nu \nabla^2 u + \mathcal{F} \quad (9)$$

where  $u$  is the fluid velocity,  $\nu$  is the fluid viscosity,  $p$  is pressure and  $\mathcal{F}$  is external force.

The idea of Navier-Stokes equation is that the earth is entirely dependent on the tenuous multi-layers of gas that cling to the surface of the globe. Variations of temperature, pressure, and moisture content in the layers of air near the earth's surface give rise to the dynamic effects known as weather.

### 3. MATHEMATICAL FORMULATION OF A MODIFIED MAXWELL'S ELECTROMAGNETIC MODEL

The weather-influenced Maxwell's electromagnetic model hinges on the following salient assumptions:

- a) The particles in each layer absorb energy, transform (electrical to kinetic energy) and excite more charges downward and
- b) The number of main channel from cloud to ground is negligible.

The charged molecules are believed to spin. We propose that the nature of excited charge spin initiates the preliminary events of lightning. We therefore introduce the time-independent Schrödinger equation to account for its spin as follows in Equation 10:

$$i\hbar \frac{\partial}{\partial t} \psi - \frac{\hbar^2}{2m} \nabla^2 \psi + V\psi = 0 \quad (10)$$

We applied the Navier-Stokes equation into the Schrödinger on the assumptions that  $\mathcal{F}$  is insignificant and  $(\mathbf{u} \cdot \nabla) \mathbf{u} = \nabla u^2 = \mathbf{u}^2 \nabla$  as shown in Equation 11:

$$ia\hbar \frac{\partial}{\partial t} \psi - b\nabla^2 \psi + Vc\psi = 0 \quad (11)$$

Here  $a = 1 + \mathbf{v} \cdot \mathbf{u} + \frac{i\hbar}{2m} \mathbf{u} \cdot \nabla$ ,  $b = u^2$ ,  $c = \mathbf{p} + \mathbf{v} \cdot \mathbf{u}$

The langrangian density related to Equation 11 is given as shown in Equation 12:

$$\mathcal{L}_1 = \frac{1}{2} \left[ a \left| \frac{\partial \psi}{\partial t} \right|^2 - b |\nabla \psi|^2 - Vc |\psi|^2 \right] \quad (12)$$

We apply the minimum coupling rule to describe the interaction of  $\psi$  with the electrostatic Field,

$$\text{i.e.} \quad \frac{\partial}{\partial t} \mapsto \frac{\partial}{\partial t} + ieV, \quad \nabla \mapsto \nabla - ieA \quad \text{where } \phi = V_o + E_o \left( \frac{y^2}{x} - x \right)$$

where  $V$  is the potential across atmospheric surfaces,  $A$  is potential across charged molecules,  $\phi$  the total potential in the system,  $V_o$  is the potential on the surface of the charged air,  $E_o$  is the electric field and  $x$  is the width of the lightning strokes,  $\left( \frac{y^2}{x} - x \right)$  is the lightning potential,  $y$  is the Dybe length. Equation 12 transforms into Equation 13:

$$\mathcal{L}_1 = \frac{1}{2} \left[ a \left| \frac{\partial \psi}{\partial t} + ie\psi\phi \right|^2 - b |\nabla \psi - ieA\psi|^2 - Vc |\psi|^2 \right] \quad (13)$$

$$\mathcal{L}_1 = \frac{1}{2} \left[ a \left| \frac{\partial \psi}{\partial t} + ie\psi V_o + iE_o e\psi \left( \frac{y^2}{x} - x \right) \right|^2 - b |\nabla \psi - ieA\psi|^2 - Vc |\psi|^2 \right] \quad (14)$$

We apply the solution of the standing wave  $\psi(x, t) = e^{iS(x,t)}T(x, t)$  in Equation 14 where  $E, B : \mathbb{R}^3 \times \mathbb{R} \rightarrow \mathbb{R}$ , the lagrangian density takes the form in Equation 15:

$$\mathcal{L}_1 = \frac{1}{2} \left\{ E_{rt}^2 - |E_z|^2 + \left[ b|eA|^2 + a|V_o e|^2 - a \left( \left| E_o e \left( \frac{y^2}{x} - x \right) \right|^2 \right) + 2aE_o V_o e^2 \right] E_r^2 \right\} \quad (15)$$

Considering the lagrangian density of the particle in an electrostatic fields  $E_1$ - $E_2$  field of the atmospheric influence where  $E_1 = E_z$  and  $E_2 = E_{rt}$  as shown in Equation 16:

$$\mathcal{L}_o = \frac{1}{2} |E_1|^2 - \frac{1}{2} |E_2|^2 \quad (16)$$

Here the total action of lagrangian density is a linear combination given as shown in Equation 17:

$$D = \mathcal{L}_1 + \mathcal{L}_o \quad (17)$$

From the basics of moving charge and the corresponding magnetic field they produced, we assumed that the charges mobility is maximum within the lightning channel i.e.  $B_{max} = \frac{\mu_o q v}{4\pi r^2}$  and  $E_{max} = \frac{1}{4\pi \epsilon_o} \frac{q}{r^2}$ . As shown in Equation 18:

$$D = B_{max}^2 \epsilon_o^2 \mu_o^2 |eA|^2 E_r^2 + a|V_o e|^2 E_r^2 E_{max}^2 - a \left( \left| E_o e \left( \frac{y^2}{x} - x \right) \right|^2 \right) E_{max}^2 E_r^2 + 2aE_o V_o e^2 E_{max}^2 E_r^2 \quad (18)$$

Since lagrangian density is calculated as the difference of kinetic and the internal energy densities (Alejandro, 2003) i.e.  $D = \frac{1}{2} m v^2 - qV$ , therefore Equation 18 becomes

$$\frac{1}{2} m v^2 - qV = B_{max}^2 \epsilon_o^2 \mu_o^2 |eA|^2 E_r^2 + a|V_o e|^2 E_r^2 E_{max}^2 - a \left( \left| E_o e \left( \frac{y^2}{x} - x \right) \right|^2 \right) E_{max}^2 E_r^2 + 2aE_o V_o e^2 E_{max}^2 E_r^2 \quad (19)$$

The calculation is as indicated in Equation 19, shown above.

This yields three governing equations as shown in Equations 20–22.

$$\frac{1}{2} m v^2 = B_{max}^2 \epsilon_o^2 \mu_o^2 |eA|^2 E_r^2 \quad (20)$$

$$-qV = a|V_o e|^2 E_r^2 E_{max}^2 + 2aE_o V_o e^2 E_{max}^2 E_r^2 \quad (21)$$

$$-a \left( \left| E_o e \left( \frac{y^2}{x} - x \right) \right|^2 \right) E_{max}^2 E_r^2 = 0 \quad (22)$$

Equations 20–22 represent the linear form of electromagnetic model and it is synonymous with Equations 1–3, i.e. the horizontal, vertical and azimuth magnetic fields of the electromagnetic model. The internal energy is the varying energy, which is influenced by atmospheric disturbances, (e.g. air pressure, temperature, energy conversion due to collision of particulates,

etc.) from the cloud through the branching point or layers (as proposed in our model) to the ground. We propose that this process be translated to the magnitude of the momentum of the return stroke. Equation 20 represents the magnetic induction as a result of the atmospheric particulate charged dynamics. It also represent the effect of the spin factor ( $\epsilon$ ) on the general lightning system. We propose that the spin factor of each particulate defines the lightning type (e.g. cloud-cloud or cloud-to-ground) and the frequency of branching from the lightning channel. Equation 21 reveals the effect of the electrical pressure on lightning transmission. This electrical pressure in this context is almost synonymous to the atmospheric pressure. An increase in the electrical pressure in the channel increases the atmospheric pressure. Perhaps the difference between both pressures is that electrical pressure is triggered by high return stroke current which heats up the channel, while the atmospheric pressure is triggered by external factors like electrical pressure, differential heating, and convective activity, etc. The atmospheric pressure initiates an increase in the number of molecules, though it occurs when the electric field exceeds the threshold energy. Electrical pressure initiates the production of new electrons in the atmosphere which exceeds their recombination rate, leading to atmospheric electrical breakdown. The potential  $V_o \approx V_o(H)$  expresses the potential at different layer heights ( $H$ ) as proposed by our model. Here, we adopt a polynomial scheme, i.e. the basic Taylor's series. Our choice of Taylor's series is based on the reliable application of the scheme in various theoretical meteorological researches (Baer & Zhang, 1998; Randall & Konor, 2008) as shown in Equation 23:

$$V_o(H) = V_o(H_o) + (H - H_o) \left( \frac{\partial V_o}{\partial H} \right)_{H_o} + \frac{(H - H_o)^2}{2!} \left( \frac{\partial^2 V_o}{\partial H^2} \right)_{H_o} + \dots \dots \dots \quad (23)$$

Here  $\left( \frac{\partial V_o}{\partial H} \right)_{H_o} = \frac{V_o(H_o + \nabla H) - V_o(H_o - \nabla H)}{2\nabla H}$

Equation 21 can be used to characterize electrically atmospheric pressure on the conditions that other weather factors, e.g. Coriolis, convective updraft, etc., are stable. Then, classical mechanics is applied as shown in Equation 24:

$$-qV = a|V_o e|^2 E_r^2 E_{max}^2 + 2aE_o V_o e^2 E_{max}^2 E_r^2 \approx H\rho g \quad (24)$$

$H$  is the vertical height from cloud to ground,  $\rho$  is the density across air layers (see Figure 1) and  $g$  is the acceleration due to gravity. Further on Equation 24, classical relationship is given as Equation 25.

$$H \approx V_o; \rho \approx e^2 E_{max}^2 E_r^2; g \approx a. \quad (25)$$

$$(H\rho g)_1 + \frac{2E_o}{V_o} (H\rho g)_2 \approx H\rho g$$

We assumed that the lightning channel is cylindrical and the values of electric and magnetic were adapted from the literature (Emetere, 2015; Glenn, 1977), i.e. as shown in Equations 26–27:

$$E_1 = \beta E_r e_r e^{-j\beta r} \sin\theta \quad (26)$$

$$E_2 = \beta E_r e_{r1} e^{-j\beta r} \cos\theta \quad (27)$$

Here,  $e_r = e_{r1} = \frac{\xi m}{4\pi r}$ ,  $e_r$  is the spin factor which determines the electron spin along the horizontal component of the channel,  $\beta$  is the frequency of excited power,  $\xi$  represents the electrical permittivity;  $\mu_o$  represents the magnetic permeability,  $r$  represents the radius or horizontal component of the channel,  $m$  is the mass of the charged particulate in the atmosphere.

The boundary conditions for Equation 26 are shown in Equation 28:

$$\begin{cases} E_1(r) = E_\alpha(H) \cdot \alpha \\ E_1(\infty) = 0 \end{cases} \quad (28)$$

The boundary conditions for Equation 27 are shown in Equation 29:

$$\begin{cases} E_2(r) = E_\gamma(H) \cdot \gamma \\ E_2(\infty) = 0 \end{cases} \quad (29)$$

$\alpha$  and  $\gamma$  are the attenuation factors of the electrical fields.

#### 4. GROUND DATA VALIDATION OF THE MODEL

In this section, the Davis Vantage Pro2 weather station was used to validate Equation 25 using the month of May for 2012 and 2013. Past research in the same location (coastal region of South-West Nigeria) where the Davis weather station is located had shown that the highest number of lightning strikes occurs in the month of May within the years ranging from 2006-2009 (Mowete & Adelabu, 2009). Figures 1a & 1b show the pressure profile, while Figure 2 show the temperature profile. Figure 3 represents the air density for the month of May for 2012 and 2013.

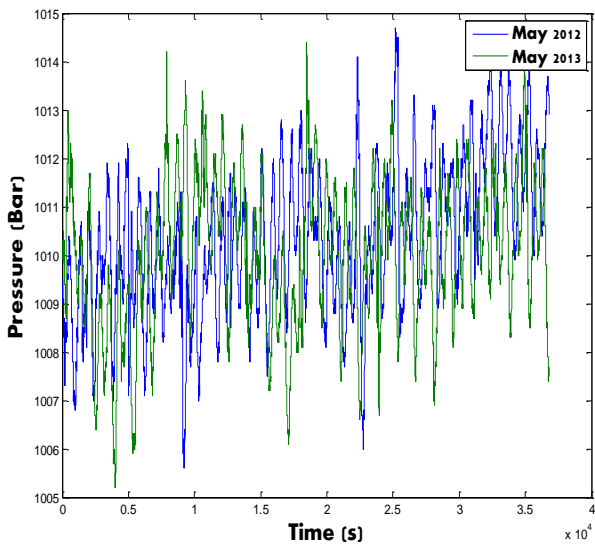


Figure 1a Pressure profile-air layers

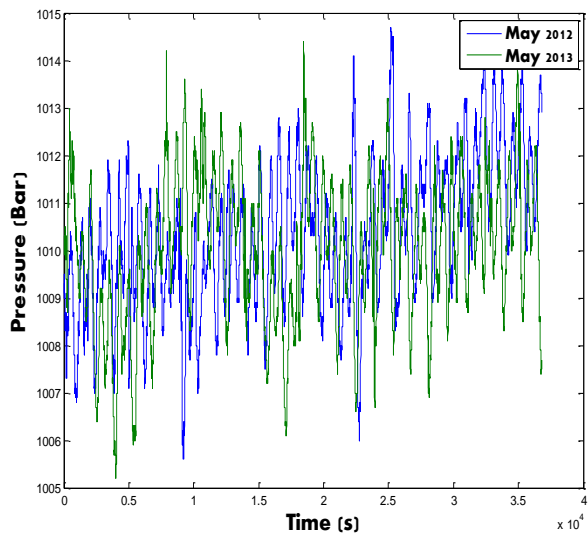


Figure 1b Pressure profile-active-site

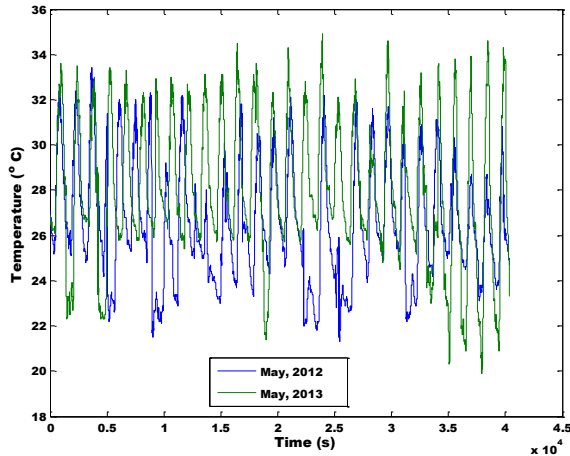


Figure 2 Temperature profile-active-site

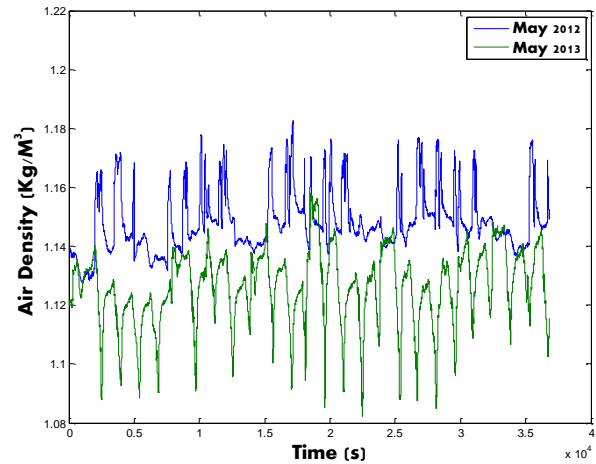


Figure 3 Air density for May, 2012 and 2013

Before lightning strikes, the temperature is inversely proportional to the pressure. This is evident in the patterns shown in Figure 1b & Figure 2 (compare the red circles on both figures). This is the basic reason of greater peaks for May, 2012 than in May, 2013. By observation, the peak values do represent the lightning occurrences (Emetere et al., 2014). Therefore, the peak of the pressure graph is directly proportional to the number of lightning occurrences. We had earlier proposed the lightning branches are as a result of varying physical parameters in the air layer. Using the idea that when three or more peaks pass through the same line (Figure 1b), they are perceived to operate at same layer, we found a minimum of ten layers, depicting the branching points of the lightning channel. The lower level ( $L_6$  to  $L_{10}$  shown in Figure 1a) is where the pressure due to the surface of the charged air  $((H\rho g)_1)$  is located while the upper ( $L_1$  to  $L_5$  shown in Figure 1a) is where the pressure, due to the charged dynamics  $\frac{2E_0}{V_0} (H\rho g)_2$ , is located. Lightning occurs at the upper pressure level (Emetere et al., 2014; Lee, 1986), while the low pressure level initiates an updraft, i.e. air rises and condenses into a cumulonimbus cloud (Huffines & Orville, 1999). We tried comparing the red circles in Figures 1 and 2 for May, 2012. Atmospheric temperature is not proportional to the pressure during a high magnitude lightning stroke (Figure 1b and Figure 2). We considered the air density at the upper pressure as shown in Figure 3. This shows the importance of  $\frac{2E_0}{V_0}$  in determining the leader stroke in lightning process.

The air density reveals the charge dynamics where low air density depicts how the Positive upward streamer rising from the ground to meet the stepped leader (see the arrows in Figure 3). This shows the importance of  $e^2 E_{max}^2 E_r^2$  in the electromagnetic model. Its full analysis is accomplished, i.e. using Equations 26–29, though other conditions could be explored depending on the research objective.

## 5. APPLICATION OF FINDINGS TO ELECTRICITY

It has been estimated that one stroke of lightning carries very high electricity. Hence, it is paramount to our findings how it is possible that the mathematical framework can describe an imaginary lightning panel (Emetere et al., 2014). The lightning panel is expected to obey Maxwell's electromagnetic model which is hinged on the following salient assumption that particulates at each layer of the lightning panel have a medium intermolecular force to allow sudden excited particulates in the panel to be translated into electricity.

Layer 'a' is the transparent coating, layer 'b' is the transparent surface, layer 'c' is the transparent anode layer, layer 'd' is the hole transport layer, layer 'e' is the photoactive layer and layer 'f' is

the hybridized cathode layer. Each arrangement is inserted into slots within the module-like solar cells. The case coating has a high thermal conductivity which harvests the excess heat into the water ways. The coordination of the very fast excited particles for layers 'c' to 'f' can be demonstrated by Equation 21 as shown in Equation 30:

$$\frac{-qV}{aV_0 e^2 E_{max}^2 E_r^2} = -V_0 + 2E_0 \quad (30)$$

From the basic concept of electromotive force, Equation 30 is further calculated in Equations 31–31:

$$\frac{-qV}{aV_0 e^2 E_{max}^2 E_r^2} = -V_0 + 2E_0 = E_0 + V \quad (31)$$

$$E_0 = -V \left( \frac{q}{aV_0 e^2 E_{max}^2 E_r^2} + 1 \right) \quad (32)$$

Equation 32 reveals a very sound mechanism to convey fast excited particulates to generate electricity in a typical lightning panel. However, further research maybe done to see the impact of the minus sign on the photoactive layer of the lightning panel.

## 6. CONCLUSION

The weather- influenced Maxwell's electromagnetic model has enabled the identification of key parameters, i.e.  $e^2 E_{max}^2 E_r^2$  and  $\frac{2E_0}{V_0}$  which are key factors for building the lightning panel for energy production using lightning. Before lightning, the temperature is inversely proportional to the pressure. During lightning, the temperature is fairly stable, though it varies between air layers. Lightning branches are a result of varying physical parameters in the air layer. Lightning occurs at the upper pressure level, while the low pressure level initiates an updraft, i.e. air rises and condenses into a cumulonimbus cloud. From the governing Equations 20–22, we have been able to explore the significance of Equation 21. The essence of the Equations 20–22 is to create a mathematical framework (Equation 32) for the construction of lightning tracking panel. Other aspects of the governing equations shall be explored extensively in further research.

## 7. ACKNOWLEDGEMENT

The authors appreciate the host institution for their partial sponsorship. The data for this paper are available on Physics Department of Covenant University Davis weather station.

## 8. REFERENCES

- Alejandro, C., 2003. Lagrangian Density Equations of Single-fluid and Two-fluid Flows. *International Journal of Heat and Technology*, Volume 21, pp. 13–20
- Baba, Y., Rakov, V.A., 2005. On the Mechanism of Attenuation of Current Waves Propagating Along a Vertical Perfectly Conducting Wire Above Ground: Application to Lightning. *IEEE Trans. Electromagnetic Compatibility*, Volume 47(3), pp. 521–532
- Baer, F., Zhang, B., 1998. Optimizing Computations in Weather and Climate Prediction Models. *Meteorology and Atmospheric Physics*, Volume 67, pp. 153–168
- Emetere, M.E., Olawole, O.F., Sanni, S.E., 2015a. Theoretical Design of Lightning Panel. *In: 2015 PIAMSEE: AIP Conference Proceedings* 1705

- Emetere, M.E., Akinyemi, M.L., Uno, U.E., 2015b. Computational Analysis of Aerosol Dispersion Trends from Cement Factory. *In: IEEE Proceedings 2015 International Conference on Space Science & Communication, Langkawi, 13 August 2015, Malaysia*
- Emetere, M.E., Akinyemi, M.L., Uno, U.E., Boyo, A.O., 2014. Lightning Threat Forecast Simulation using the Schrodinger-Electrostatic Algorithm. *IERI Procedia*, Volume 9(1), pp. 53–58
- Emetere, M.E., 2015. The Physics of Investigating the Sheath Effect on the Resultant Magnetic Field of a Cylindrical Monopole Plasma Antenna Institute of Physics. *Plasma Science and Technology*, Volume 17(2), pp. 153–158
- Glenn, S.S., 1977. Efficiency of Electrically Small Antennas Combined with Matching Network. *IEEE Trans Antennas and Propagation*, Volume 25, pp. 369–373
- Hussein, A., Milewski, M., Janischewskyj, W., Noor, F., Jabbar, F., 2007. Characteristics of Lightning Flashes Striking the CN Tower below Its Tip. *Journal of Electrostatics*, Volume 65, pp. 307–315
- Huffines, G.R., Orville, R.E., 1999. Lightning Ground Flash Density and Thunderstorm Duration in the Contiguous United States. *Journal of Applied Meteorology*, Volume 38, pp. 1013–1019
- Lee, R.H., 1986. The Shattering Effect of Lightning-Pressure from Heating of Air by Stroke Current, Industry Applications. *IEEE Transactions on Industry Applications*, Volume 22, pp. 416–419
- Lupo, G., Petrarca, C., Tucci, V., Vitelli, M., 2000. EM Fields Associated with Lightning Channels: On the Effect of Tortuosity and Branching. *IEEE Transaction on Electromagnetic Compatibility*, Volume 42, pp. 394–404
- Miller, E.K., Poggio, A.J., Burke, G.J., 1973. An Integro-differential Equation Technique for the Time-domain Analysis of Thin Wire Structures. *Journal of Computational Physics*, Volume 12, pp. 24–48
- Mowete, A.I., Adelabu, M.A.K., 2009. An Assessment of Lightning and other Electrostatic Disturbances along the Coast of South West Nigeria. *In: XIX-th International Conference on Electromagnetic Disturbances*, pp. 200–203
- Rachidi, F., Bermudez, J., Rubinstein, M., Rakov, V., 2004. On the Estimation of Lightning Peak Currents from Measured Fields using Lightning Location Systems. *Journal of Electrostatics*, Volume 60, pp. 121–129
- Rakov, V.A., Uman, M.A., 1998. Review and Evaluation of Lightning Return Stroke Models Including some Aspects of their Application. *IEEE Transactions on Electromagnetic Compatibility*, Volume 40(4), pp. 403–426
- Randall, D., Konor, C., 2008. Simulation of Global Cloudiness. *Journal of Physics: Conference Series*, Volume 125(012021), pp. 1–5
- Schoene, J., Uman, M.A., Rakov, V.A., Rambo, K.J., Jerauld, J., Schnetzer, G.H., 2003. Test of the Transmission Line Model and the Traveling Current Source Model with Triggered Lightning Return Strokes at Very Close Range. *Journal of Geophysical Research*, Volume 108(D23), pp. 1–14
- Srivastava, A.K., Tripathi, S.N., 2010. Numerical Study for Production of Space Charge within the Stratiform Cloud. *Journal of Earth System Science*, Volume 119, pp. 627–638
- Tatematsu, A., Noda, T., Yokoyama, S., 2004. Simulation of Lightning Induced Voltages on a Distribution Line using the FDTD Method. *International Workshop on High Voltage Engineering*, The Institute of Electrical Engineers of Japan
- Uman, M.A., McLain, D.K., 1969. Magnetic Field of the Lightning Return Stroke. *Journal of Geophysical Research*, Volume 74, pp. 6899–6910

Ziegler, C.L., MacGorman, D.R., 1994. Observed Lightning Morphology Relative to Modeled Space Charge and Electric Field Distributions in a Tornadic Storm. *Journal of the Atmospheric Sciences*, Volume 51, pp. 833–851